Tetrahedron 68 (2012) 830–840

Contents lists available at SciVerse ScienceDirect

Tetrahedron

journal homepage: www.elsevier.com/locate/tet

Synthesis of non-covalent BODIPY–metalloporphyrin dyads and triads

Tamanna K. Khan, Mangalampalli Ravikanth *

Department of Chemistry, Indian Institute of Technology Bombay, Powai, Mumbai 400 076, India

ARTICLE INFO

Article history:
Received 23 September 2011
Received in revised form 16 November 2011
Accepted 18 November 2011
Available online 25 November 2011

Keywords:
Boron-dipyrromethenes
Metalloporphyrins
Metal–pyridyl coordination
BODIPY–metalloporphyrin assemblies

ABSTRACT

Boron-dipyrromethenes (BODIPY) containing oxypyridine substituents at 3- and 3,5-positions and metalloporphyrins (Zn(II), Ru(II)) were used to synthesize four non-covalent BODIPY–metalloporphyrin dyads and four BODIPY–metalloporphyrin triads assembled using metal–pyridine 'N' interaction. The formation of BODIPY–metalloporphyrin assemblies was confirmed by 1D and 2D NMR methods and X-ray crystal structure obtained for one of the BODIPY–metalloporphyrin dyad. In ^{1}H NMR, the signals of oxypyridine group(s) of BODIPY unit showed significant upfield shifts supporting the coordination of oxypyridine group of BODIPY unit to metalloporphyrin unit. The NMR study also indicated that Zn(II) porphyrin forms relatively weak BODIPY–Zn(II) porphyrin conjugates, whereas Ru(II) porphyrin forms strong BODIPY–Ru(II) porphyrin conjugates. The X-ray structure solved for BODIPY–Zn(II)porphyrin dyad revealed that the Zn(II) porphyrin coordinated to the BODIPY unit obliquely and the angle between the Zn(II) porphyrin and the pyridyl ring is 70°. The absorption properties of stable BODIPY–Ru(II) porphyrin conjugates showed the overlapping absorption features of both the components and the fluorescence studies indicated that the BODIPY unit emission was significantly quenched on coordination with **RuTPP**(CO) unit. The electrochemical studies exhibited the features of both BODIPY and metalloporphyrin units in dyads and traids.

1. Introduction

The metal–pyridine interactions play a very important role in generating supramolecular architectures that include squares, macrocycles, catenanes, cages, and tubes.[1–5] Most of these metal–pyridine based supramolecular structures were shown to be stable both in solution and solid state and are characterized thoroughly by NMR and X-ray crystallography.[6,7] The prime advantage of using pyridine is that it is one of the versatile ligand, which can form complexes with various transition metal ions. Our group is interested in the design and synthesis of new boron-dipyrromethene dyes for various applications.[8–11] Boron-dipyrromethenes (4,4-difluoro-4-bora-3a,4a-diaza-*s*-indacene, BODIPY) are excellent fluorophores and have been used in various research fields as labeling reagents, fluorescent switches, chemosensors, light harvesting systems, and dye sensitized solar cells because of their advantageous photophysical properties, such as photostability, high absorption coefficients, and high fluorescence quantum yields.[12–14] BODIPY dyes are amenable to modifications, which allow fine tuning of properties by introduction of suitable substituents at appropriate positions of the dipyrromethene framework. There are several positions on BODIPY chromophore where substituents can be introduced to tune the electronic properties. Recently Dehaen and co-workers[15–19] reported the synthesis of 3,5-dihalo functionalized BODIPYs, which gives an access to synthesize a wide range of 3,5-disubstituted BODIPYs containing oxygen, carbon, nitrogen, and sulfur centered nucleophiles. We adopted this approach and treated 3,5-dibromo BODIPYs with 2-, 3-, and 4-hydroxypyridines in CH_3CN in the presence of Cs_2CO_3 under very mild conditions.[20] The 2- and 4-hydroxypyridines on reaction with 3,5-dibromo BODIPYs in the presence of base in CH_3CN at refluxing temperature afforded 3,5-bis(pyridone)BODIPYs, whereas 3-hydroxypridine under same reaction conditions with 3,5-dibromo BODIPY gave 3,5-bis(oxypyridine)BODIPYs. These two classes of BODIPYs are different from each other in their spectral, electrochemical, and photophysical properties significantly.[20] Although, the 3,5-bis(oxypyridine) BODIPYs did not show much alteration in properties compared to the reference 3,5-unsubstituted *meso*-aryl boron-dipyrromethene,[21] these BODIPYs containing decorated oxypyridine groups are very useful building blocks to synthesize BODIPY–metalloporphyrin conjugates by using non-covalent metal–pyridine interactions, which is explored in this paper. A simple stoichiometric reaction between BODIPY with oxypyridine substituents and metalloporphyrin (Zn^{II} and Ru^{II}) resulted in the formation of BODIPY–metalloporphyrin assemblies **5**–**12** in high yields. 1D, 2D NMR, and X-ray crystallography techniques were used to confirm the formation of BODIPY–metalloporphyrin dyads **5**–**8** and triads **9**–**12**. The spectral and electrochemical properties indicated that the BODIPY

* Corresponding author. Tel.: +91 022 2576 7176; fax: +91 022 2576 7152; e-mail address: ravikanth@chem.iitb.ac.in (M. Ravikanth).

0040-4020/$ – see front matter © 2011 Elsevier Ltd. All rights reserved.
doi:10.1016/j.tet.2011.11.048

and metalloporphyrin components interact weakly and retain their individual characteristic features in these assemblies.

2. Results and discussion

The mono- and dioxypyridine substituted *meso*-aryl BODIPY building blocks **1**–**4** used for the synthesis of non-covalent BODIPY–metalloporphyrin assemblies are shown in the Chart 1. The 3,5-di(oxypyridine) *meso*-anisyl BODIPY **3** and 3,5-di(oxypyridne) *meso*-furyl BODIPY **4** were synthesized by following our earlier reported method.[20] The mono oxypyridinyl substituted BODIPYs, 3-(oxypyridine) *meso*-anisyl BODIPY **1** and 3-(oxypyridine) *meso*-furyl BODIPY **2** were prepared by treating 1 equiv of the corresponding 3-bromo BODIPYs **13** and **14**, respectively[9] with 1 equiv of 3-hydroxypyridine in CH_3CN in the presence of Cs_2CO_3 at refluxing temperature for 1 h. The crude reaction mixtures were purified by silica gel column chromatography and afforded mono oxypyridinyl substituted *meso*-aryl BODIPYs **1** and **2** in 60–70% yields. The compounds **1** and **2** are freely soluble in common organic solvents and confirmed by molecular ion peak in HRMS mass spectra and clean ^1H, ^{19}F, and ^{11}B NMR spectra. The absorption and fluorescence properties of compounds **1**–**4** are in line with the general behavior of pyrrole unsubstituted *meso*-aryl BODIPY, such as *meso*-phenyl boron dipyrromethene[21] indicating that the oxypyridine substituent(s) at 3- and 3,5-positions did not alter the electronic properties of BODIPY core.

The compounds **1**–**4** containing one and two oxypyridine substituents at 3- or 3,5-positions were used as building blocks to construct supramolecular architectures by treating them with metalloporphyrins, such as **ZnTPP** and **RuTPP**(CO)(EtOH). The non-covalent dyads, such as **5**–**8** were synthesized as shown in the Scheme 1. The dyads **5** and **6** were synthesized by treating **1** and **2**, respectively, with 1 equiv of **ZnTPP** in $CHCl_3$ for 30 min at room temperature and the crude compounds were recrystallized using $CHCl_3$/*n*-hexane. The dyads **5** and **6** are not stable for column chromatographic purification on silica indicating that the components BODIPY and **ZnTPP** are weakly bonded in these dyads. On the other hand, the dyads **7** and **8** were prepared by reacting 1 equiv of **1** and **2**, respectively, with 1 equiv of **RuTPP**(CO)(EtOH) at 80 °C for overnight. The progress of the reaction was followed by TLC analysis. The crude reaction mixtures were subjected to column chromatographic purification on silica using petroleum ether/dichloromethane and afforded the red colored dyads **7** and **8** in 55–70% yields.

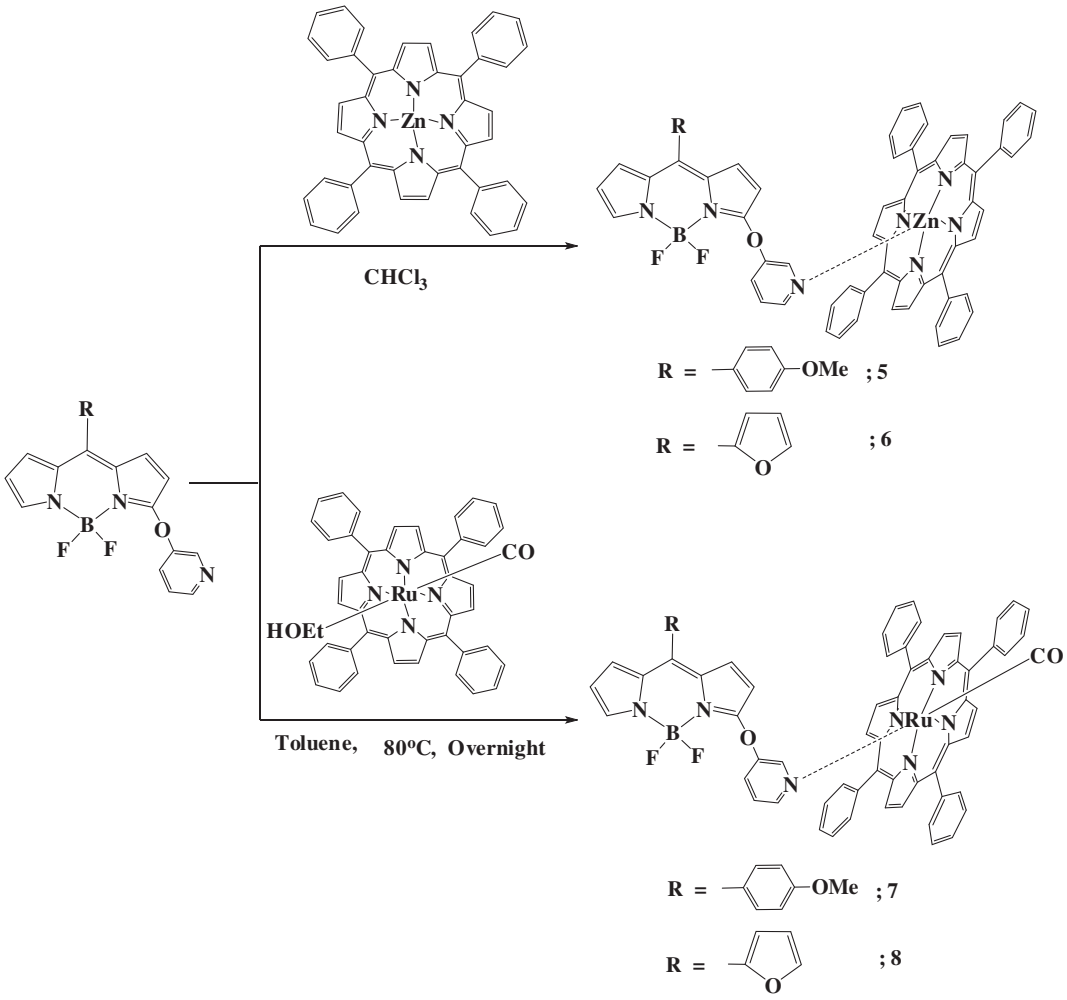

Scheme 1. Synthesis of dyads **5**–**8**.

The dyads **5**–**8** were confirmed by molecular ion peak in ES-MS mass spectra. However, the formation of all four dyads **5**–**8** were unambiguously confirmed by a detailed 1D and 2D NMR studies. The comparison of ^1H NMR spectra of dyads **5** and **7** and a BODIPY building block **1** is shown in Fig. 1a along with proton assignments. The assignments were made on the basis of the resonance position and intensity data as well as the proton-to-proton connectivity revealed in the ^1H–^1H COSY spectrum shown for dyad **6** in Fig. 1b. The relevant ^1H NMR data of all BODIPY–metalloporphyrin dyads

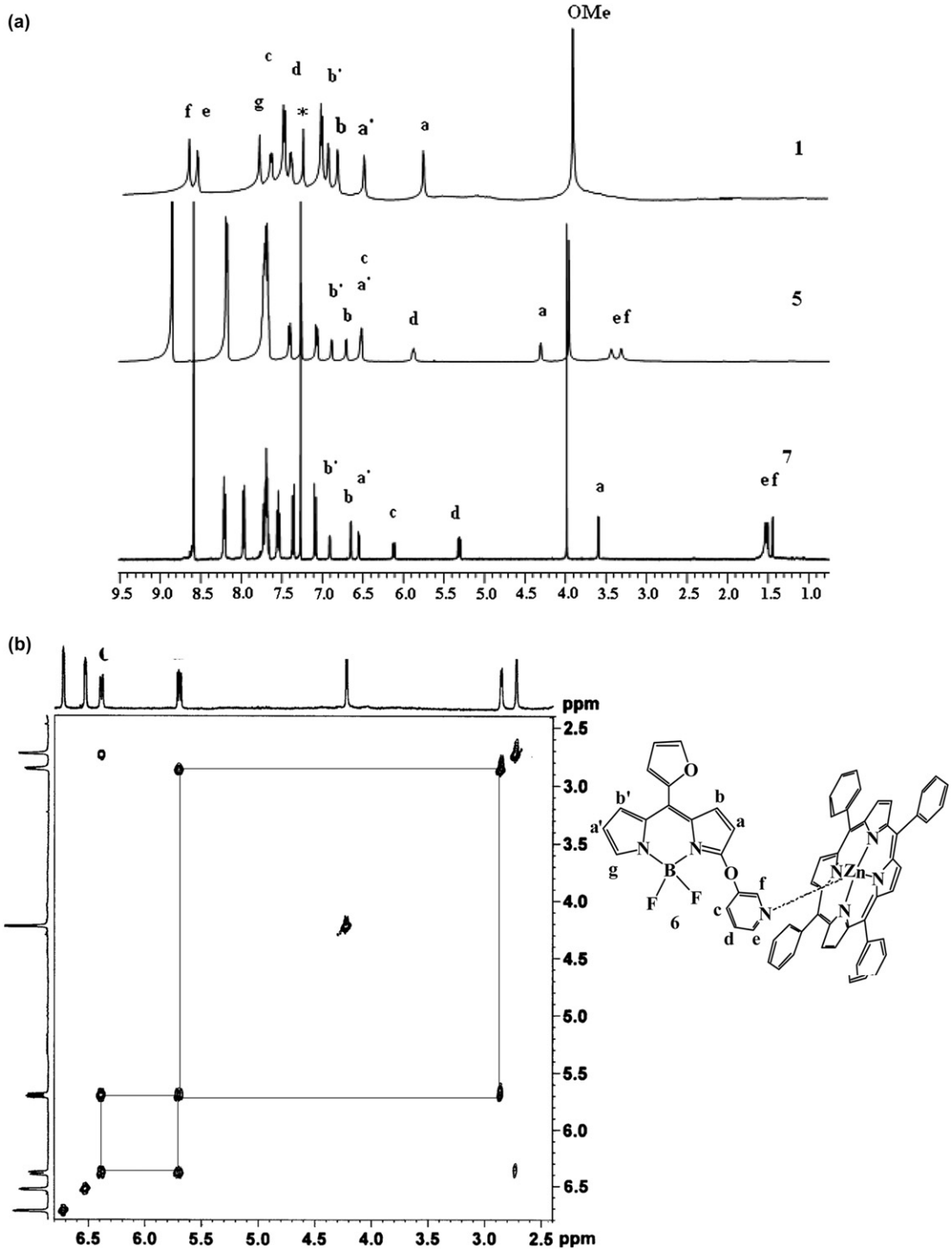

Fig. 1. (a) Comparison of ^{1}H NMR spectra for compounds **5**, **7**, and **1** (b) ^{1}H–^{1}H COSY-NMR spectrum for compound **6** in selected region recorded in $CDCl_3$.

and the corresponding monomers are presented in Table 1. In ^{1}H NMR, the signals corresponding to both the components, BODIPY and metalloporphyrin are present with alterations in their chemical shifts. In ^{1}H NMR, the metalloporphyrin component resonances in the dyads **5**–**8** did not show much changes in their chemical shifts compared to corresponding monomeric metalloporphyrins but the significant changes in the chemical shifts were observed for BODIPY units because of ring current effect of metalloporphyrin, which cause changes in chemical shifts of protons located near its plane. As clear from the Fig. 1b and data in Table 1, the pyridyl protons, which are closer to porphyrin ring experienced significant upfield shifts compared to pyrrole protons of BODIPY core. It is noted that only type a pyrrole proton experienced 1–2 ppm upfield shift, whereas all other pyrrole protons of BODIPY core did not show any shift. On the other hand, the pyridyl protons of type c–f, which were identified by the proton connectivity pattern in ^{1}H–^{1}H COSY spectra experienced significant upfield shifts compared to the pyridyl protons of the free BODIPY building block. For example, in the dyad **5**, the porphyrin ring current shift of BODIPY protons of type c–f is $\Delta\delta=\delta$ (dyad **5**)$-\delta$ (free BODIPY **1**), which is ~5.1 for type e,f-protons and ~1.1 ppm for type c,d-protons.

Table 1
^{1}H NMR chemical shift values (in ppm) for compounds **1**–**10** recorded in $CDCl_3$

Sr. no.	a	b	a′	b′	g	f1	f2	f3	c	d	e	f
1	5.76 (d)	6.68 (s)	6.51 (s)	6.94 (d)	7.80 (s)				7.65 (d)	7.39–7.43 (m)	8.56 (d)	8.67 (s)
5	4.29 (d)	6.69 (d)	6.50 (s)	6.87 (d)	7.65–7.75 (m)				6.50 (s)	5.85–5.88 (m)	3.43 (s)	3.30 (s)
7	3.56 (d)	6.63 (d)	6.55 (s)	6.90 (d)	7.65–7.72 (m)				6.10 (d)	5.29 (m)	1.48 (d)	1.41 (s)
2	5.81 (d)	7.28 (d)	6.68 (s)	7.49 (d)	7.81 (s)	7.07 (d)	6.54–6.52 (m)	7.81 (s)	7.65–7.67 (m)	7.40–7.43 (m)	8.57 (d)	8.67 (d)
6	4.24 (d)	7.17 (d)	6.52–6.53 (m)	7.32 (d)	7.69 m	6.99 (d)	6.72 (s)	7.82 (s)	6.39 (d)	5.70–5.74 (m)	2.93 (d)	2.72 (d)
8	3.66 (d)	7.15 (d)	6.56–6.57 (m)	7.36 (d)	7.67–7.74 (m)	6.99 (d)	6.75 (m)	7.85 (s)	6.10 (d)	5.29–5.33 (m)	1.48 (d)	1.44 (d)
3	5.74 (d)	6.81 (d)							7.63 (d)	7.36 (d)	8.52 (s)	8.66 (s)
9	4.27 (d)	6.60 (d)							6.40 (d)	5.79–5.8 (m)		3.20 (br s)
11	3.56 (d)	6.56 (d)							6.10 (d)	5.23–5.29 (m)		1.43 (s)
4	5.79 (d)	7.30 (d)				6.97 (d)	6.65–6.67 (m)	7.75 (s)	7.62 (m)	7.36 (d)	8.52 (d)	8.65 (d)
10	4.62 (d)	7.10 (d)				6.85 (d)	6.73 (s)	7.81 (s)	6.62 (d)	6.07–6.1 (m)		4.23 (br s)
12	3.66 (d)	7.04 (d)				6.81 (d)	6.78 (s)	7.87 (s)	5.98 (d)	5.22–5.26 (dd)		1.42–1.45 (m)

The significant shift observed for type e,f-protons is because of their close proximity to the metalloporphyrin ring compared to type c,d-protons. Similar observations were made for BODIPY-**RuTPP**(CO) dyads **7** and **8**. However, in BODIPY–**RuTPP**(CO) dyads **7** and **8**, the pyridyl protons of type c,d, ($\Delta\delta = \sim 1.5$) and type e,f ($\Delta\delta = \sim 7.1$) experienced more upfield shifts compared to dyads **5** and **6** supporting that the BODIPY and **RuTPP**(CO) units were bonded more strongly in these dyads (Supplementary data).

The BODIPY–metalloporphyrin triads **9**–**12** (Chart 2) were also synthesized by adopting the same approach used for dyads **5**–**8**. The triads **9**–**12** showed the corresponding molecular ion peak in ES-MS mass spectra confirming their identities. Further confirmation for the formation of triads **9**–**12** was obtained by detailed 1D and 2D NMR studies (Supplementary data). Because of the symmetric arrangement, the ^{1}H NMR spectra of triads **9**–**12** are very simple unlike dyads **5**–**8**. A systematic titration of **ZnTPP** with BODIPY **3** was carried out in $CDCl_3$ and the changes in the ^{1}H NMR are shown in Fig. 2a. The **ZnTPP** equivalents were varied gradually from 0 to 2 equiv and the changes observed in the ^{1}H NMR clearly supports the formation of triad **9**. As clear from the Fig. 2a, on increasing the addition of **ZnTPP** to BODIPY **3** up to 2 equiv, the pyrrole protons of type 'a' and pyridyl protons of type c–f steadily experiences upfield shift and maximum shifts were observed on complete addition of 2 equiv of **ZnTPP** confirming the formation of triad **9**. This was also confirmed by recording 1D and 2D NMR spectra for the triad **9**, which was isolated by treating 1 equiv of BODIPY **3** with 2 equiv of **ZnTPP** in $CHCl_3$ at room temperature followed by recrystallization (Fig. 2b). The triads **11** and **12**, which were isolated by column chromatography also showed similar upfield shifts of pyridyl protons. However, the pyridyl protons appeared at more upfield because of strong coordination of Ru(II)-pyridyl 'N' in these triads (Supplementary data). Thus, 1D and 2D NMR studies clearly supported the formation of dyads **5**–**8** and triads **9**–**12**.

We fortunately obtained the crystal structure of dyad **6**, which confirmed the formation of this kind of BODIPY–metalloporphyrin dyads **5**–**8** and triads **9**–**12**. The single crystals of dyad **6** and its corresponding free BODIPY monomer **2** were obtained from *n*-hexane/dichloromethane on slow evaporation over a period of one week. Both compounds crystallized in the triclinic crystal system with the same $P-1$ space group. Fig. 3 shows the crystal structures of compounds **2** and **6** and the important bond lengths and angles are presented in Table 2. In compound **2**, the two pyrrole rings and the six membered ring containing boron are almost in the same plane like any other BODIPY dye.[21] However, in compound **6**, because of Zn(II)porphyrin coordination with the oxypyridine group of BODIPY, the two pyrrole rings (planes 4 and 5) are not in one plane and they are oriented at 15° with each other (Supplementary data).The six membered boron containing ring in compound **6** is distorted and the boron atom is slightly deviated from the main dipyrrin framework. The angle between the plane defining *meso*-furyl ring (plane 2) and the plane defining various dipyrrin atoms (plane 1) in compound **2** is ~31°, which is almost remained same (~33°) in compound **6**. It has been shown recently that the *meso*-furyl ring, because of its smaller size orients more toward the boron dipyrrin ring resulting in the decrease of the dihedral angle compared to *meso*-aryl substituted BODIPYs.[22] Furthermore, in compound **2**, the plane 3 defining pyridyl group is at an angle of 82° w.r.t. boron-dipyrrin (plane 1), which is substantially reduced to 42° in compound **6** because of the coordination of pyridyl 'N' with Zn(II) porphyrin. The angle between pyridyl plane 3 and plane 6 defining porphyrin ring is 70° indicating that pyridyl group is not completely perpendicular to the plane of the metalloporphyrin. The Zn-pyridyl 'N' bond length is 2.21 Å, which is in the same range as those of similar systems reported earlier.[23–25] The Zn atom lies slightly above the basal plane defined by the four nitrogen atoms (plane 6) with the deviation of 0.308 Å.

There are also slight alterations in bond lengths and bond angles in compound **6** w.r.t. compound **2** due to coordination of BODIPY pyridyl 'N' with Zn(II)porphyrin.

Since the BODIPY–**ZnTPP** based dyads **5**/**6** and triads **9**/**10** are not stable at low concentration, the absorption properties of only the stable BODIPY–**RuTPP**(CO) based dyads **7**/**8** and triads **11**/**12** and their corresponding monomers were studied in $CHCl_3$ and the data are presented in Table 3. The comparison of dyad **7** and triad **11** recorded at the same concentration in $CHCl_3$ is shown in Fig. 4a. In general, the pyridyl substituted boron–dipyrromethene complexes[20] **1**–**4** show a strong absorption band corresponding to $S_0 \rightarrow S_1$ transition in 500–540 nm region and **RuTPP**(CO)(EtOH) exhibits one strong Soret band at 413 nm and two weak Q-bands at 530 and 570 nm. As clear from the Fig. 4a and the data presented in Table 3 that the dyads **7**/**8** and triads **11**/**12** showed bands corresponding to both the components with negligible variation in their peak maxima compared to their corresponding monomers. The emission properties of dyads **7**/**8** and triads **11**/**12** were studied by steady state fluorescence technique and relevant data are included in Table 3. The comparison of steady state fluorescence spectra of triad **11** and BODIPY monomer **3** recorded in $CHCl_3$ using excitation wavelength of 488 nm is shown in Fig. 4b. The BODIPY monomer **3** is decently fluorescent with a quantum yield of 0.58. However, in triad **11**, the BODIPY fluorescence was quenched by 93%. Similarly, the BODIPY emission in dyads **7**/**8** and triad **12** was also quenched significantly. These results indicated that the ruthenium ion, which coordinated to pyridyl 'N' of BODIPY unit quenches the singlet state of the BODIPY unit by enhancing the spin-forbidden deactivation processes.

The electrochemical properties of dyads **5**–**8** and triads **9**–**12** along with their corresponding monomers were followed by cyclic voltammetry in CH_2Cl_2 using tetrabutylammonium perchlorate as a supporting electrolyte. A comparison of cyclic voltammograms of dyad **5** and its constituted monomers **1** and **ZnTPP** is shown in Fig. 5 and data are presented in Table 4. In dyads **5**–**8** and triads **9**–**12**, we observed three reductions corresponding to BODIPY and

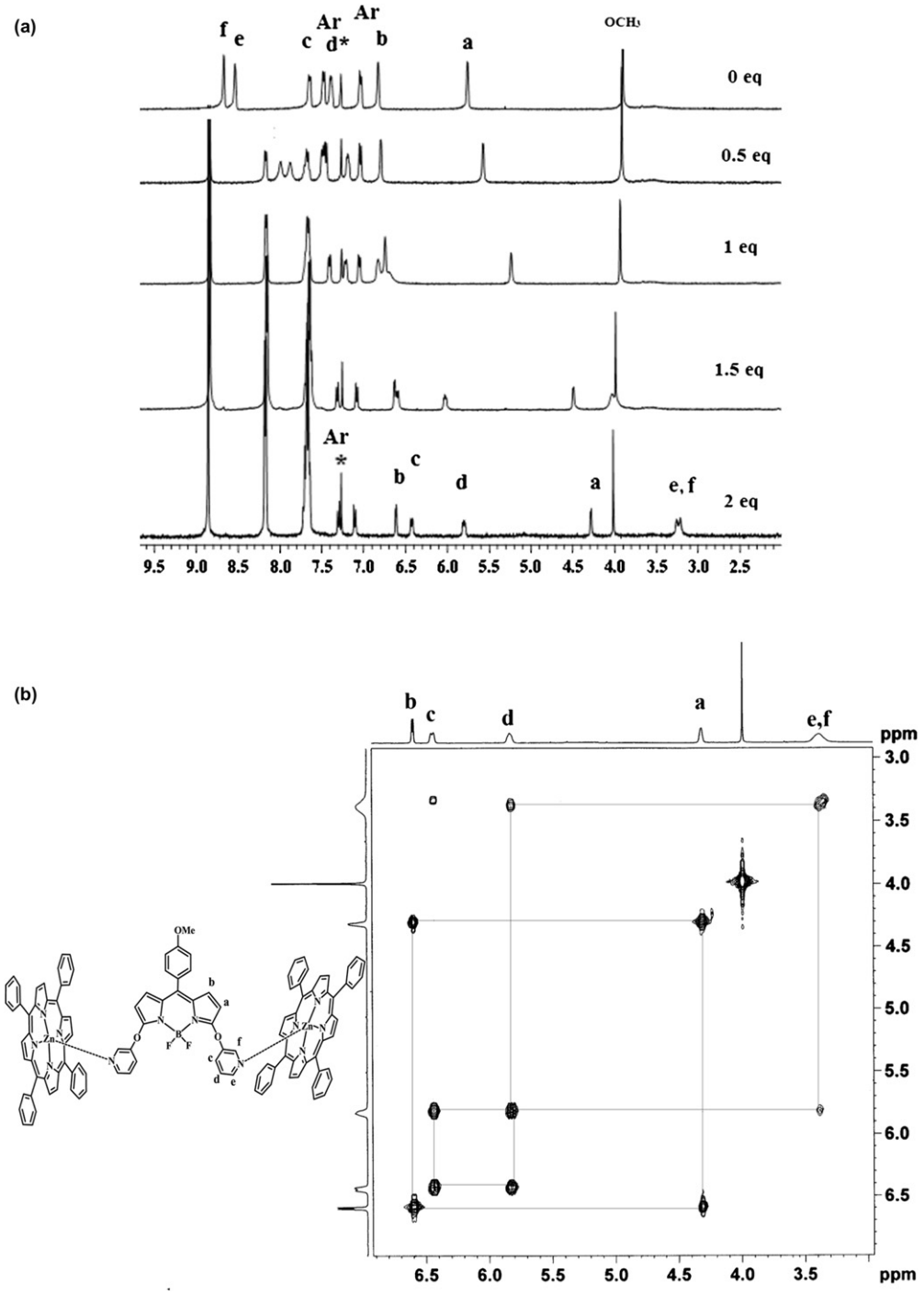

Fig. 2. (a) ^{1}H NMR titration of **3** with addition of increasing equivalents of **ZnTPP** (0–2 equiv). (b) ^{1}H–^{1}H COSY NMR spectrum of compound **9** in selected region recorded in $CDCl_3$.

metalloporphyrin units and two oxidations corresponding to only metalloporphyrin unit. For example, the dyad **5** showed three reductions at −0.85, −1.23, and −1.68 V and two oxidations at 0.80 and 1.1 V. The first reduction at −0.85 V was due to BODIPY unit **1** and the two reductions and two oxidations were because of **ZnTPP** unit. A close inspection of data of dyads **5**–**8** and triads **9**–**12** indicate that the potentials of dyads **5**–**8** and triads **9**–**12** were in the same range of their constituted monomers. Thus, the electrochemical studies of dyads **5**–**8** and triads **9**–**12** indicate that the BODIPY and metalloporphyrin sub-units in dyads and triads interact very weakly.

3. Conclusions

Four BODIPY–metalloporphyrin dyads **5**–**8** and four BODIPY–metalloporphyrin triads **9**–**12** were synthesized by treating BODIPYs containing oxypyridine substituents at 3- and 3,5-positions, respectively, with metalloporphyrins (Zn(II) and Ru(II)) utilizing pyridine–metalloporphyrin interaction. The formation of dyads **5**–**8** and triads **9**–**12** were confirmed by significant upfield shifts of pyridyl protons due to the ring current effect of metalloporphyrin. The NMR study also revealed that BODIPY-**RuTPP**(CO) dyads **7**/**8** and triads **11**/**12** are more stable than BODIPY-**ZnTPP**

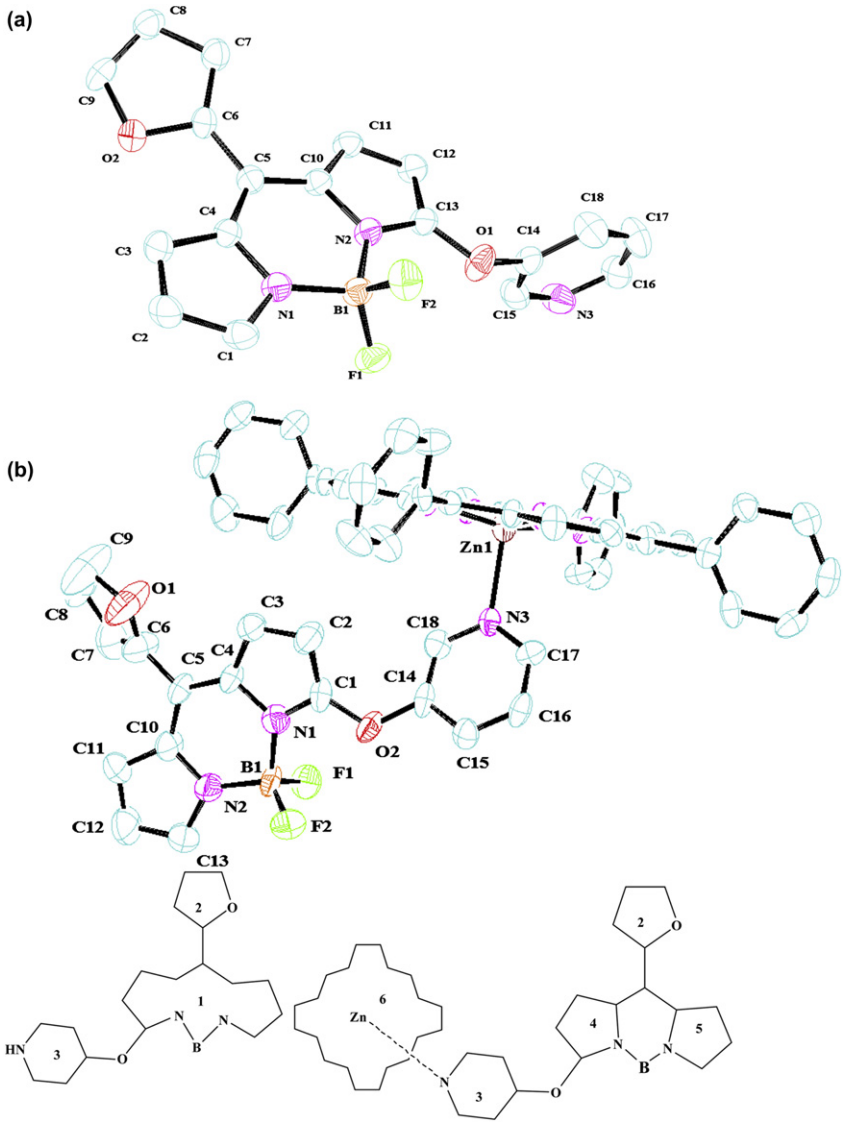

Fig. 3. X-ray crystal structures of compounds (a) **2** and (b) **6**. Selected mean planes for the compound **2** and **6** also shown at the bottom.

dyads **5**/**6** and triads **9**/**10**. The X-ray structure obtained for BODIPY-Zn(II)porphyrin dyad **5** indicated that the BODIPY unit in conjugate **5** is slightly distorted compared to free BODIPY and it is obliquely oriented with metalloporphyrin unit. The absorption and electrochemical studies indicated that the conjugates exhibit features of both the constituted monomeric units. The emission of BODIPY unit in dyads and triads was significantly quenched because of **RuTPP**(CO) unit, which enhances the non-radiative deactivation processes.

Table 2
Selected bond distances (Å) and bond angles (°) for compounds **2** and **6**

Bond Length/Torsion angles	**2**	**6**
B1–N1	1.53	1.57
B1–N2	1.55	1.51
B1–F1	1.38	1.41
B1–F2	1.39	1.37
F1–B1–F2	108.46	108.87
N1–B1–N2	106.28	106.18
C6–O1–C9	106.22	111.29
C1–O2–C14/C13–O2–C14	117.71	120.08
C(2)–H(2)	0.95	0.95
C4–C5–C10	120.16	119.47
C17–N3–C18	116.01	119.93
O(1)–C(6)–C(5)–C(4)	31.6	33.4
Zn–N3	—	2.21
Zn–N4	—	2.05 (4)
Zn–N5	—	2.02 (5)
Zn–N6	—	2.07 (4)
Zn–N7	—	2.04 (5)
Zn displacement	—	0.308 (5)

Table 3
Photophysical data for dyads **7**/**8** and triads **11**/**12** along with their reference compounds recorded in $CHCl_3$

Compound	λ_{abs} (nm)	λ_{em} (nm)	Φ_F BODIPY	(%Q)[a]
1	504 (4.7)	521	0.10	—
2	526 (4.7)	573	0.11	—
3	516 (4.9)	537	0.58	—
4	538 (4.5)	583	0.15	—
RuTPP	413 (5.5), 531 (4.5), 569 (sh)	—	—	—
7	413 (5.4), 505 (4.9), 534 (4.3), 569 (sh)	521	0.028	70%
8	413 (5.3), 531 (4.5), 569 (sh)	570	0.033	70%
11	413 (5.5), 518 (4.9), 568 (sh)	537	0.035	93%
12	413 (5.6), 535 (4.8), 570 (sh)	583	0.028	81%

[a] (%Q) denotes percentage of quenching of fluorescence quantum yield of BODIPY unit.

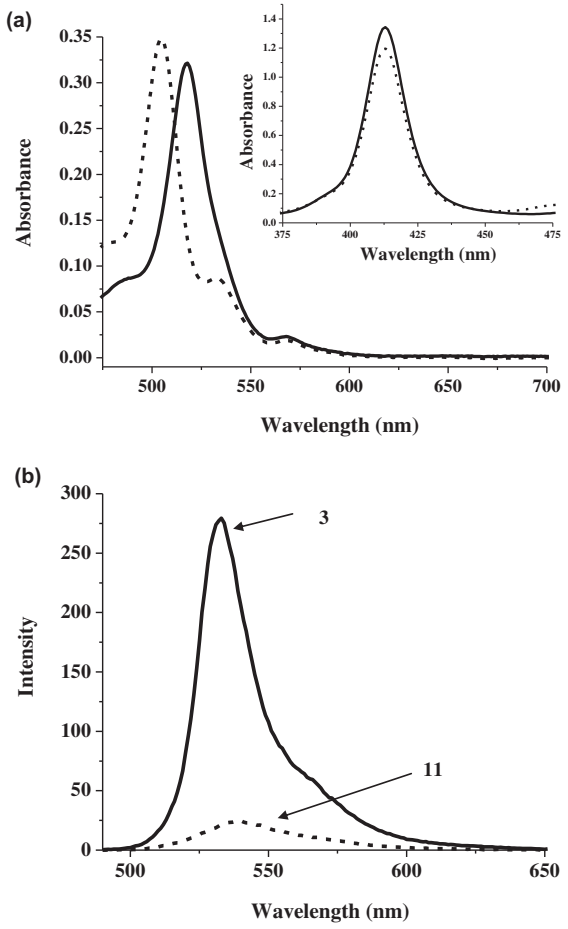

Fig. 4. A comparison of Q and Soret band (inset) absorption spectra of dyad **7** (—) and triad **11** (—) recorded in $CHCl_3$. The concentration used for Q-band was 1×10^{-5} M and for Soret band was 1×10^{-6} M. (b) Comparison of emission spectra of BODIPY monomer **3** (—) and triad **11** (—) at λ_{ex} 488 nm recorded in $CHCl_3$.

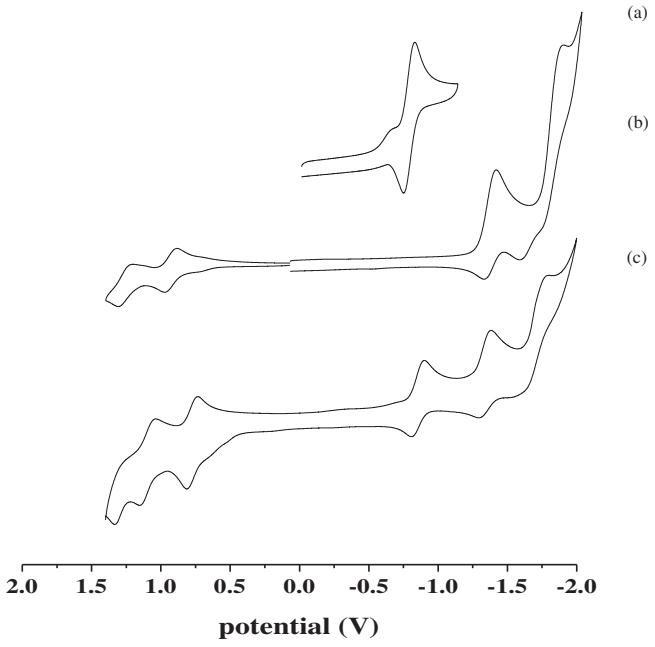

Fig. 5. Comparison of cyclic voltammograms (a) **1**, (b) **ZnTPP**, and (c) **5** in dichloromethane containing 0.1 M TBAP as supporting electrolyte recorded at 50 mV/s scan speed.

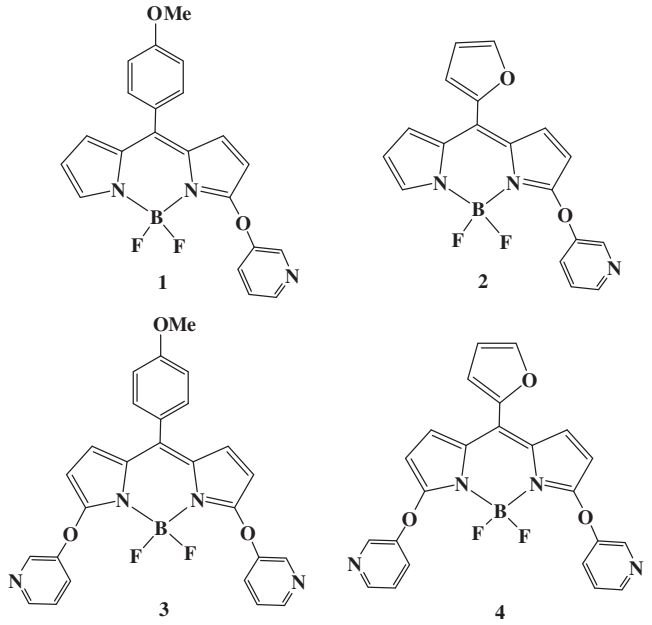

Chart 1. Structures of compounds **1**–**4**.

4. Experimental section

4.1. Chemicals

The known compounds **3** and **4**, were prepared by following the literature method.[20] Compounds **13** and **14** were prepared by following the reported procedures.[9] THF and toluene were dried over sodium benzophenone ketyl and chloroform dried over calcium hydride prior to use. $BF_3{\cdot}OEt_2$ and 2,3-dichloro-5,6-dicyano-1,4-benzoquinone (DDQ) obtained from Spectrochem (India) were used as obtained. All other chemicals used for the synthesis were reagent grade unless otherwise specified. Column chromatography was performed on silica (60–120 mesh) or alumina.

4.2. Instrumentation

^{1}H NMR spectra (δ in ppm) were recorded using Varian VXR 300, 400 MHz and Bruker 400 MHz spectrometer. ^{13}C NMR spectra were recorded on Bruker operating at 100.6 MHz ^{19}F NMR spectra were recorded on Bruker operating at 376.4 MHz ^{11}B NMR spectra were recorded on Bruker operating at 128.3 MHz. TMS was used as an internal reference for recording ^{1}H (of residual proton; δ 7.26) and ^{13}C (δ 77.0 signal) in $CDCl_3$. Absorption and steady state fluorescence spectra were obtained with Perkin–Elmer Lambda-35. Fluorescence spectra were recorded at 25 °C in a 1 cm quartz fluorescence cuvette. The fluorescence quantum yields (Φ_F) were estimated from the emission and absorption spectra by comparative method at the excitation wavelength of 488 nm using Rhodamine 6G (Φ_f=0.88)[18] for compounds **7**/**8** and **11**/**12** as standard. Cyclic voltammetric (CV) and differential pulse voltammetric (DPV) studies were carried out with electrochemical system utilizing the three electrode configuration consisting of a glassy carbon (working electrode), platinum wire (auxillary electrode), and saturated calomel (reference electrode) electrodes. The experiments were done in dry dichloromethane using 0.1 M tetrabutylammonium perchlorate as supporting electrolyte. Half wave potentials were measured using DPV and also calculated manually by taking the average of the cathodic and anodic peak potentials. The ES-MS mass spectra were recorded with a Q-Tof micro mass spectrometer. High-

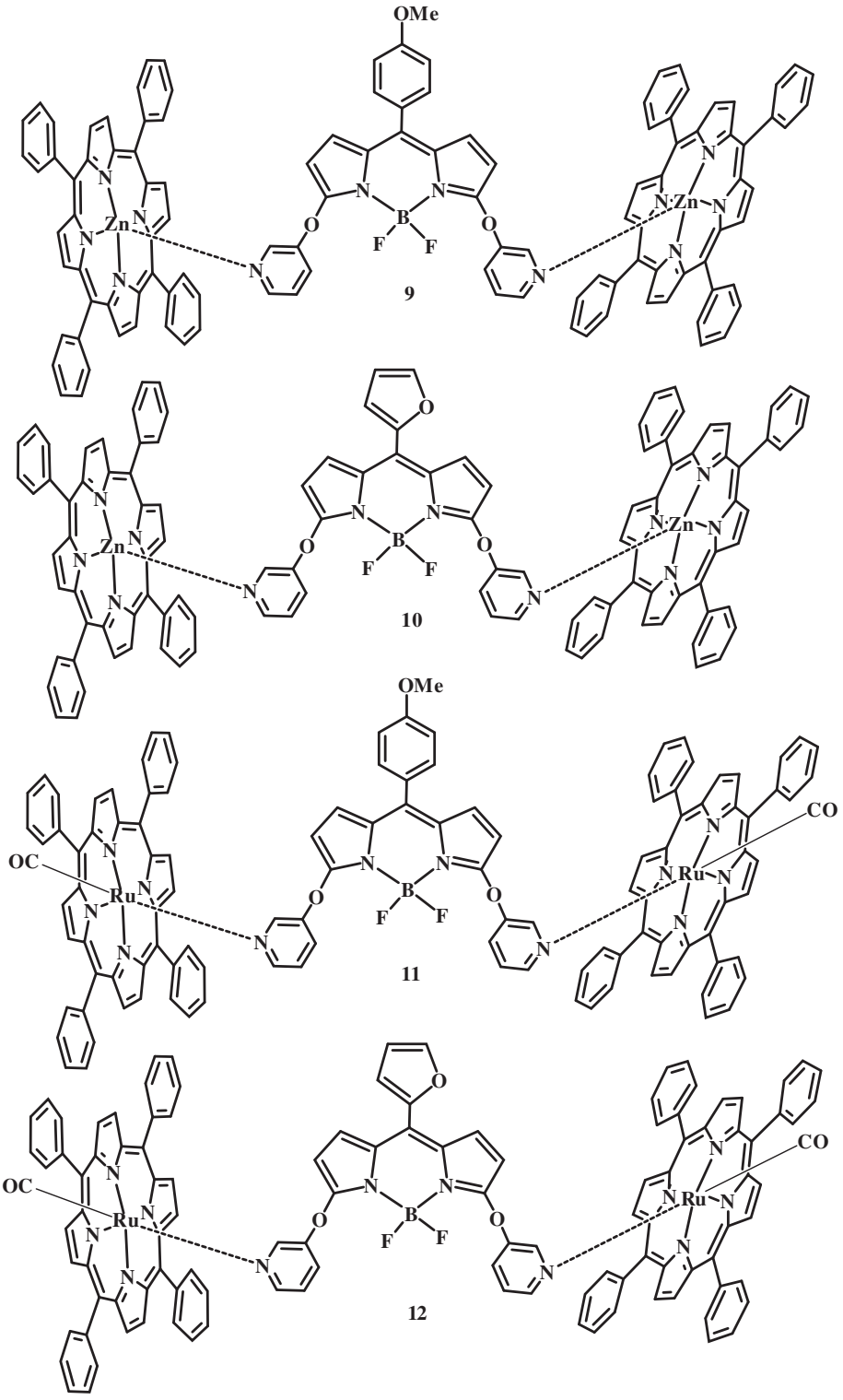

Chart 2. Structures of triads **9**–**12**.

resolution mass spectrum was obtained from Q-TOF instrument by electron spray ionization (ESI) technique.

4.3. X-ray diffraction studies

The *.cif files were deposited with the Cambridge Crystallographic Data Centre and the following codes were allocated: **2** (CCDC-824841) and **6** (CCDC-824842). The single crystals of compounds **2** and **6** were obtained on slow evaporation of *n*-hexane/dichloromethane over a period of one week. The intensity data collection for compounds **6** and **2** have been carried out on a Nonius MACH3 four circle diffractometer at 293 K. Structure solutions for the compounds **6** and **2** were obtained using direct methods (SHELXS-97)[26] and refined using full-matrix least-squares methods on F^2 using SHELXL-97.[27] Compound **2** crystallizes with two molecules in the asymmetric unit. There are no

Table 4
Electrochemical data for compounds **1**–**12** recorded in dichloromethane containing 0.1 M TBAP as supporting electrolyte recorded at 50 mV/s scan speed

Compound	Oxidation		Reduction		
	I	II	I	II	III
3	1.28		−0.913	—	−1.53
4	1.25		−0.789	—	−1.69
1	—	—	−0.888	—	—
2	—	—	−0.672	—	—
ZnTPP	0.77	1.08	—	−1.35	−1.71
RuTPP	0.870	1.43	—	—	−1.59
5	0.800	1.11	−0.852	−1.32	−1.68
6	0.800	1.11	−0.720	−1.34	−1.70
7	0.916	1.42	−0.896	—	−1.54
8	0.908	1.40	−0.708	—	−1.52
9	0.796	1.08	−0.860	−1.32	−1.70
10	0.792	1.14	−0.724	−1.34	−1.70
11	0.920	1.42	−0.972	—	−1.56
12	0.912	1.41	−0.768	—	−1.49

statistically significant differences in the metrical parameters for the two molecules.

*4.3.1. 3-(3-Oxypyridine)-8-(4-methoxyphenyl)-4,4-difluoro-4-bora-3a,4a-diaza-s-indacene **1**.* The compound **1** was synthesized by treating the 3-bromo boron dipyrromethene **13** (100 mg, 0.26 mmol) with 3-hydroxypyridine (38 mg, 0.39 mmol) in CH_3CN (15 mL) in the presence of Cs_2CO_3 (129 mg, 0.39 mmol) under nitrogen atmosphere at refluxing temperature for 1 h. The progress of the reaction was followed by TLC analysis, which showed the disappearance of starting precursors and appearance of new spot corresponding to the desired compound. The crude compound was subjected to silica gel column chromatography using petroleum ether/CH_2Cl_2 (20:80) and afforded compound **1** as orange solid in 70% yield (72 mg). R_f (20% pet. ether/CH_2Cl_2) 0.43; IR (KBr, cm^{-1}) 668, 706, 838, 982, 1030, 1122, 1215, 1356, 1443, 1560, 1605, 1749, 2840, 3019; ^{1}H NMR (400 MHz, $CDCl_3$, δ in ppm): 3.90 (3H, s, OMe), 5.76 (1H, d, J=4.0 Hz, β-py), 6.51 (1H, s, β-py), 6.68 (1H, s, β-py), 6.94 (1H, d, J=4.0 Hz, β-py), 7.02 (2H, d, J=8.0 Hz, BODIPY Ar), 7.39–7.43 (1H, m, pyridyl), 7.49 (2H, d, J=8.0 Hz, BODIPY Ar), 7.65 (1H, d, J=7.31 Hz, pyridyl), 7.80 (1H, s, β-py), 8.56 (1H, d, J=4.0 Hz, pyridyl), 8.67 (1H, s, pyridyl). ^{19}F NMR (376.4 MHz, CDCl3, δ in ppm): −147.6 (q, J_{B-F}=56.4 Hz). ^{11}B NMR (128.3 MHz, $CDCl_3$, δ in ppm): 0.24 (t, J_{B-F}=28.2 Hz). ^{13}C NMR (100 MHz, $CDCl_3$, δ in ppm): 55.62, 104.68, 114.14, 116.99, 124.61, 125.90, 128.17, 128.24, 129.77, 132.24, 133.69, 134.07, 139.91, 142.82, 144.37, 147.61, 151.18, 161.80, 165.18. HRMS mass calcd for $C_{21}H_{16}BF_2N_3O_2$ 392.1380 found 392.1382 $[M+1]^+$.

*4.3.2. 3-(3-Oxypyridine)-8-(2-furyl)-4,4-difluoro-4-bora-3a,4a-diaza-s-indacene **2**.* Compound **2** was prepared by treating 3-bromo boron dipyrromethene **14** (100 mg, 0.29 mmol) with 3-hydroxypyridine (42 mg, 0.44 mmol) under same reaction conditions mentioned for compound **1** and obtained as green solid in 61% yield (63 mg). R_f (25% pet. ether/CH_2Cl_2) 0.48; IR (KBr, cm^{-1}) 667, 701, 892, 932, 1084, 1123, 1296, 1356, 1443, 1475, 1560, 1605, 2840, 3017; ^{1}H NMR (400 MHz, $CDCl_3$, δ in ppm): 5.81 (1H, d, J=4.5 Hz, β-py), 6.54 (1H, m, f2), 6.68 (1H, s, β-py), 7.07 (1H, d, J=3.3 Hz, f1), 7.28 (1H, d, J=3.9 Hz, β-py), 7.40–7.43 (1H, m, pyridyl), 7.49 (1H, d, J=4.5 Hz, py), 7.65–7.67 (1H, m, pyridyl), 7.81 (2H, s, f3+β-py), 8.57 (1H, d, J=4.8 Hz, pyridyl), 8.67 (1H, d, J=2.7 Hz, pyridyl). HRMS mass calcd for $C_{18}H_{12}BF_2N_3O_2$ 352.1056 found 352.1069 $[M+1]^+$. ^{19}F NMR (376.4 MHz, $CDCl_3$, δ in ppm): −149.12 (q, J_{B-F}=26.3 Hz). ^{11}B NMR (128.3 MHz, $CDCl_3$, δ in ppm): 0.11 (t, J_{B-F}=28.2 Hz). ^{13}C NMR (100 MHz, $CDCl_3$, δ in ppm): 104.99, 113.14, 117.04, 118.81, 124.68, 127.41, 128.02, 128.32, 130.33, 131.08, 134.07, 139.70, 142.88, 146.95, 147.69, 148.47, 151.26, 165.13.

4.4. General synthesis for dyads 5, 6 and triads 9, 10

The dyads **5**/**6** and triads **9**/**10** were synthesized by treating 1 equiv of appropriate BODIPY (**1**–**4**) with one and 2 equiv, respectively, of **ZnTPP** in $CHCl_3$ and stirred under inert atmosphere at room temperature for 30 min. The solvent was removed on rotary evaporator under vacuo and the crude solids were recrystallized twice from $CHCl_3$/*n*-hexane to afford purple crystalline solids in 55–70% yields.

*4.4.1. Dyad **5**.* The compound **5** was obtained as purple solid in 68% yield. IR (KBr, cm^{-1}) 668, 701, 771, 1027, 1121, 1217, 1441, 3019; ^{1}H NMR (400 MHz, $CDCl_3$, δ in ppm): 3.30 (1H, s, pyridyl), 3.43 (1H, s, pyridyl), 3.95 (3H, s, OMe), 4.29 (1H, d, J=3.9 Hz, β-py), 5.85–5.88 (1H, m, pyridyl), 6.50 (2H, s, β-py+pyridyl), 6.69 (1H, d, J=4.5 Hz, β-py), 6.87 (1H, d, J=3.3 Hz, β-py), 7.05 (2H, d, J=7.3 Hz, BODIPY Ar), 7.38 (2H, d, J=7.9 Hz, BODIPY Ar), 7.65–7.75 (13H, m, Ar–N4+β-py), 8.16 (8H, d, J=7.3 Hz, Ar–N4), 8.84 (8H, s, β-py-**ZnTPP**). ^{19}F NMR (376.4 MHz, $CDCl_3$, δ in ppm): −147.48 (q, J_{B-F}=56.4 Hz). ^{11}B NMR (128.3 MHz, $CDCl_3$, δ in ppm): 0.24 (t, J_{B-F}=29.5 Hz). ^{13}C NMR (100 MHz, $CDCl_3$, δ in ppm): 55.64, 103.98, 114.18, 117.33, 120.85, 123.18, 125.80, 126.49, 127.35, 127.43, 128.83, 129.28, 131.92, 132.32, 133.79, 134.78, 135.94, 140.59, 143.43, 144.83, 149.57, 150.19, 161.88, 162.36. ES-MS mass calcd for $C_{65}H_{44}BF_2N_7O_2Zn$ 1068.65 found 1068.70 $[M]^+$.

*4.4.2. Dyad **6**.* The compound **6** was obtained as purple solid in 65% yield. IR (KBr, cm^{-1}) 669, 701, 776, 1022, 1125, 1213, 1445, 3019; ^{1}H NMR (400 MHz, $CDCl_3$, δ in ppm): 2.72 (1H, d, J=2.1 Hz, pyridyl), 2.93 (1H, d, J=4.3 Hz, pyridyl), 4.24 (1H, d, J=4.3 Hz, β-py), 5.70–5.74 (1H, m, pyridyl), 6.39 (1H, d, J=8.3 Hz, pyridyl), 6.52–6.53 (1H, m, β-py), 6.72 (1H, s, f2), 6.99 (1H, d, J=3.0 Hz, f1), 7.17 (1H, d, J=4.3 Hz, β-py), 7.32 (1H, d, J=3.9 Hz, β-py), 7.69 (13H, m, Ar–N4+β-py), 7.82 (1H, s, f3), 8.17 (8H, d, J=6.5 Hz, Ar–N4), 8.81 (8H, s, β-py-**ZnTPP**). ^{19}F NMR (376.4 MHz, $CDCl_3$, δ in ppm): −149.12 (q, J_{B-F}=26.3 Hz). ^{11}B NMR (128.3 MHz, $CDCl_3$, δ in ppm): 0.11 (t, J_{B-F}=28.2 Hz). ^{13}C NMR (100 MHz, $CDCl_3$, δ in ppm): 104.28, 113.22, 117.34, 119.15, 121.01, 123.20, 126.57, 127.44, 128.01, 131.13, 132.00, 133.64, 134.74, 135.86, 140.30, 140.69, 143.29, 147.15, 150.25. ES-MS mass calcd for $C_{62}H_{40}BF_2N_7O_2Zn$ 1028.41 found 1028.43 $[M]^+$.

*4.4.3. Triad **9**.* The compound **9** was obtained as purple crystalline solid in 70% yield. IR (KBr, cm^{-1}) 666, 700, 772, 1026, 1120, 1215, 1445, 3020; ^{1}H NMR (400 MHz, $CDCl_3$, δ in ppm): 3.20 (4H, br s, pyridyl), 4.01 (3H, s, −OMe), 4.27 (2H, d, J=4.0 Hz, β-py), 5.79 (2H, m, pyridyl), 6.40 (2H, d, J=8.5 Hz, pyridyl), 6.60 (2H, d, J=4.58 Hz, β-py), 7.09 (2H, d, J=8.5 Hz, BODIPY Ar), 7.28 (2H, d, J=8.2 Hz, BODIPY Ar), 7.64–7.70 (24H, m, Ar–N4), 8.16 (16H, d, J=6.7 Hz, Ar–N4), 8.85 (16H, s, β-py-N4). ^{19}F NMR (376.4 MHz, $CDCl_3$, δ in ppm): −149.16 (q, J_{B-F}=26.3 Hz). ^{11}B NMR (128.3 MHz, $CDCl_3$, δ in ppm): 0.34 (t, J_{B-F}=26.9 Hz). ^{13}C NMR (100 MHz, $CDCl_3$, δ in ppm): 55.62, 104.68, 114.14, 116.99, 124.61, 125.90, 128.17, 128.24, 129.77, 132.24, 133.69, 134.07, 139.91, 142.82, 144.37, 147.61, 151.18, 161.80, 165.18. ES-MS mass calcd for $C_{111}H_{71}BF_2N_{12}O_3Zn_2$ 1800.21 found 1800.24 $[M]^+$.

*4.4.4. Triad **10**.* The compound **10** was obtained as purple crystalline solid in 66% yield. IR (KBr, cm^{-1}) 667, 702, 773, 1029, 1122, 1215, 1443, 3019; ^{1}H NMR (400 MHz, $CDCl_3$, δ in ppm): 4.23 (4H, s, pyridyl), 4.62 (2H, d, J=4.02 Hz, β-py), 6.07–6.10 (2H, m, pyridyl), 6.62 (2H, d, J=7.3 Hz, pyridyl), 6.73 (1H, s, f2), 6.85 (1H, d, J=2.9 Hz, f1), 7.10 (2H, d, J=4.02 Hz, β-py), 7.61–7.69 (24H, m, Ar–N_4), 7.81 (1H, s, f3), 8.14 (16H, d, J=6.6 Hz, Ar–N_4), 8.83 (16H, s, β-py-N_4). ^{19}F NMR (376.4 MHz, $CDCl_3$, δ in ppm): −149.19 (q, J_{B-F}=56.4 Hz) ^{11}B NMR

(128.3 MHz, $CDCl_3$, δ in ppm): 0.35 (t, J_{B-F}=28.2 Hz). ^{13}C NMR (100 MHz, $CDCl_3$, δ in ppm): 102.8, 112.4, 117.2, 124.18, 124.5, 126.0, 127.3, 127.7, 130.2, 142.1, 142.5, 146.0, 146.7, 151.4, 162.2. ES-MS mass calcd for $C_{114}H_{75}BF_2N_{12}O_3Zn_2$ 1840.95 found 1841.95 $[M+1]^+$.

4.5. General synthesis for dyads 7, 8 and triads 11, 12

The dyads **7**/**8** and triads **11**/**12** were synthesized by heating the mixture of appropriate BODIPY (**1**–**4**) with 1 and 2 equiv, respectively, of **RuTPP**(CO)(EtOH) at 80 °C for 24 h under nitrogen atmosphere. The progress of the reaction was followed by TLC analysis, which showed almost complete disappearance of starting precursors and indication of formation of required dyads **7**/**8** and triads **11**/**12**. The crude compounds were subjected to silica gel column chromatographic purification using petroleum ether/CH_2Cl_2 (4:6) and afforded dyads **7**/**8** and triads **11**/**12** as red solids in ~60% yields.

4.5.1. Dyad ***7****.* The compound **7** was obtained as red solid in 59% yield. R_f (50% pet. ether/CH_2Cl_2) 0.50; IR (KBr, cm^{-1}) 668, 758, 928, 1130, 1215, 1951, 2927, 3019; ^1H NMR (400 MHz, $CDCl_3$, δ in ppm): 1.41 (1H, s, pyridyl), 1.48 (1H, d, J=5.1 Hz, pyridyl), 3.56 (1H, d, J=4.3 Hz, β-py), 3.97 (3H, s, OMe), 5.29–5.32 (1H, m, pyridyl), 6.10 (1H, d, J=8.3 Hz, pyridyl), 6.55 (1H, s, β-py), 6.63 (1H, d, J=4.3 Hz, β-py), 6.90 (1H, d, J=3.1 Hz, β-py), 7.07 (2H, d, J=8.3 Hz, BODIPY Ar), 7.33 (2H, d, J=8.3 Hz, BODIPY Ar), 7.51–7.55 (8H, m, Ar–N4), 7.65–7.72 (17H, m, Ar–N4+β-py), 7.95 (8H, d, J=7.13 Hz, Ar–N4), 8.18 (8H, d, J=6.34 Hz, Ar–N4), 8.58 (16H, s, β-py-N4). ^{19}F NMR (376.4 MHz, $CDCl_3$, δ in ppm): −147.6 (q, J_{B-F}=56.4 Hz). ^{11}B NMR (128.3 MHz, $CDCl_3$, δ in ppm): 0.24 (t, J_{B-F}=28.2 Hz). ^{13}C NMR (100 MHz, $CDCl_3$, δ in ppm): 55.73, 103.40, 114.21, 117.25, 121.75, 122.43, 125.83, 126.50, 126.67, 127.43, 128.58, 129.38, 132.05, 132.30, 133.80, 134.24, 134.36, 137.57, 140.37, 141.50, 142.60, 143.76, 144.66, 148.39, 161.91, 162.64. ES-MS mass calcd for $C_{66}H_{44}BF_2N_7O_3Ru$ 1133.26 found 1134.72 $[M+1]^+$; HRMS mass calcd 1134.2688 found 1134.2679 $[M+1]^+$.

4.5.2. Dyad ***8****.* The compound **8** was obtained as red solid in 58% yield. R_f (55% pet. ether/CH_2Cl_2) 0.44; IR (KBr, cm^{-1}) 668, 702, 757, 928, 1130, 1216, 1306, 1427, 1949, 2927, 3019; ^1H NMR (400 MHz, $CDCl_3$, δ in ppm): 1.44 (1H, d, J=2.6, pyridyl), 1.48 (1H, d, J=5.4 Hz, pyridyl), 3.66 (1H, d, J=4.5 Hz, β-Py), 5.29–5.33 (1H, m, pyridyl), 6.10 (1H, d, J=8.0 Hz, pyridyl), 6.56–6.57 (1H, m, β-py), 6.75 (1H, m, f1), 6.99 (1H, d, J=3.1 Hz, f2), 7.15 (2H, d, J=4.6 Hz, β-py), 7.36 (1H, d, J=3.5 Hz, β-py), 7.54–7.65 (8H, m, Ar–N4), 7.67–7.74 (17H, m, Ar–N4+β-py), 7.85 (1H, s, f3), 7.95 (8H, d, J=7.5 Hz, Ar–N4), 8.15–8.19 (8H, m, Ar–N4), 8.59 (16H, s, β-py-N4). ^{19}F NMR (376.4 MHz, $CDCl_3$, δ in ppm): −149.10 (q, J_{B-F}=26.3 Hz). ^{11}B NMR (128.3 MHz, $CDCl_3$, δ in ppm): 0.12 (t, J_{B-F}=28.2 Hz). ES-MS mass calcd for $C_{63}H_{40}BF_2N_7O_3Ru$ 1093.23 found 1094.28 $[M+1]^+$; HRMS mass calcd 1093.2297 found 1093.2264 $[M]^+$.

4.5.3. Triad ***11****.* The compound **11** was obtained as red solid in 62% yield. R_f (65% pet. ether/CH_2Cl_2) 0.38; IR (KBr, cm^{-1}) 669, 758, 928, 1130, 1216, 1950, 2927, 3019; ^1H NMR (400 MHz, $CDCl_3$, δ in ppm): 1.43 (4H, s, pyridyl), 3.56 (2H, d, J=4.02 Hz, β-py), 5.23–5.29 (2H, m, pyridyl), 6.01 (2H, d, J=8.8 Hz, pyridyl), 6.56 (2H, d, J=4.58 Hz, β-py), 7.09 (2H, d, J=7.8 Hz, BODIPY Ar), 7.16 (2H, d, J=7.6 Hz, BODIPY Ar), 7.49 (8H, d, J=6.84 Hz, Ar–N4), 7.63–7.76 (16H, m, Ar–N4), 7.90 (8H, d, J=6.6 Hz, Ar–N4), 8.17 (8H, d, J=6.6 Hz, Ar–N4), 8.55 (16H, s, β-py-N4). ^{19}F NMR (376.4 MHz, $CDCl_3$, δ in ppm): −149.38 (q, J_{B-F}=56.4 Hz). ^{11}B NMR (128.3 MHz, $CDCl_3$, δ in ppm): 0.39 (t, J_{B-F}=29.5 Hz). ^{13}C NMR (100 MHz, $CDCl_3$, δ in ppm): 22.6, 55.82, 101.62, 114.25, 121.75, 122.36, 125.12, 125.49, 126.47, 126.66, 127.41, 128.01, 128.42, 129.23, 131.07, 132.03, 132.21, 134.21, 134.38, 134.98, 137.40, 141.20, 142.67, 143.78, 148.59, 160.60, 180.48. ES-MS mass calcd for $C_{116}H_{75}BF_2N_{12}O_5Ru_2$ 1968.41 found 1969.52 $[M+1]^+$; HRMS mass calcd 1969.4210 found 1969.4236 $[M+1]^+$.

4.5.4. Triad ***12****.* The compound **12** was obtained as red solid in 60% yield. R_f (75% pet. ether/CH_2Cl_2) 0.40; IR (KBr, cm^{-1}) 668, 702, 757, 1008, 1130, 1216, 1427, 1596, 1949, 2854, 2926, 3019; ^1H NMR (400 MHz, $CDCl_3$, δ in ppm): 1.42–1.45 (4H, m, pyridyl), 3.66 (2H, d, J=4.7 Hz, β-py), 5.22–5.26 (2H, dd, J^1=J^2=8.2 Hz, pyridyl), 5.98 (2H, d, J=8.2 Hz, pyridyl), 6.78 (1H, s, f2), 6.81 (1H, d, J=3.5 Hz, f1), 7.04 (2H, d, J=4.3 Hz, β-py), 7.49–7.52 (8H, m, Ar–N4), 7.62–7.72 (16H, m, Ar–N4), 7.87 (1H, s, f3), 7.90 (8H, d, J=7.4 Hz, Ar–N4), 8.16 (8H, d, J=7.1 Hz, Ar–N4), 8.56 (16H, s, β-py-N4). ^{19}F NMR (376.4 MHz, $CDCl_3$, δ in ppm): −149.46 (q, J_{B-F}=56.4 Hz). ^{11}B NMR (128.3 MHz, $CDCl_3$, δ in ppm): 0.57 (t, J_{B-F}=27.3 Hz). ^{13}C NMR (100 MHz, $CDCl_3$, δ in ppm): 102.90, 112.98, 117.98, 120.81, 123.53, 126.10, 126.45, 127.28, 129.03, 130.67, 131.89, 134.81, 137.52, 142.28, 143.54, 146.63, 147.86, 150.19, 150.42, 160.86 ES-MS mass calcd for $C_{113}H_{71}BF_2N_{12}O_5Ru_2$ 1928.80 found 1928.81 $[M]^+$; HRMS mass calcd 1929.3897 found 1929.3907 $[M+1]^+$.

Acknowledgements

M.R. thanks Department of Atomic Energy (DAE) for financial support and T.K.K. thanks Indian Institute of technology for the fellowship. We thank the DST-funded National Single Crystal X-ray Diffraction Facility for diffraction data.

Supplementary data

Copies of mass, NMR, absorption, fluorescence spectra, cyclic voltammograms of selected compounds, and X-ray crystallographic data of compounds **2** and **6** in CIF format. Supplementary data associated with this article can be found, in the online version, at doi:10.1016/j.tet.2011.11.048.

References and notes

1. Imamura, T.; Fukushima, K. *Coord. Chem. Rev.* **2000**, *198*, 133–156.
2. Wojaczynski, J.; Latos-Grazynski, L. *Coord. Chem. Rev.* **2000**, *204*, 113–171.
3. Beletskaya, I.; Tyurin, V. S.; Tsivadze, A. Y.; Guilard, R.; Stern, C. *Chem. Rev.* **2009**, *109*, 1659–1713.
4. Tashiro, K.; Aida, T. *Chem. Soc. Rev.* **2007**, *36*, 189–197.
5. Stulz, E.; Scott, S. M.; Bond, A. D.; Teat, S. J.; Sanders, J. K. M. *Chem.—Eur. J.* **2003**, *9*, 6039–6048.
6. Iengo, E.; Zangrando, E.; Alessio, E. *Eur. J. Inorg. Chem.* **2003**, 2371–2384.
7. Metselaar, G. A.; Ballester, P.; de Mendoza, J. *New J. Chem.* **2009**, *33*, 777–783.
8. Rao, M. R.; Mobin, S. M.; Ravikanth, M. *Tetrahedron* **2010**, *66*, 1728–1734.
9. Rajeswara Rao, M.; Kumar, K. V. P.; Ravikanth, M. *J. Organomet. Chem.* **2010**, *695*, 863–869.
10. Rajeswara Rao, M.; Bolligarla, R.; Butcher, R. J.; Ravikanth, M. *Inorg. Chem.* **2010**, *49*, 10606–10616.
11. Madhu, S.; Rao, M. R.; Shaikh, M. S.; Ravikanth, M. *Inorg. Chem.* **2011**, *50*, 4392–4400.
12. Loudet, A.; Burgess, K. *Chem. Rev.* **2007**, *107*, 4891–4932.
13. Ziessel, R.; Ulrich, G.; Harriman, A. *New J. Chem.* **2007**, *31*, 496–501.
14. Ulrich, G.; Ziessel, R.; Harriman, A. *Angew. Chem., Int. Ed.* **2008**, *47*, 1184–1201.
15. Baruah, M.; Qin, W.; Basarić, N.; De Borggraeve, W. M.; Boens, N. *J. Org. Chem.* **2005**, *70*, 4152–4157.
16. Baruah, M.; Qin, W.; Vallée, R. A. L.; Beljonne, D.; Rohand, T.; Dehaen, W.; Boens, N. *Org. Lett.* **2005**, *7*, 4377–4380.
17. Qin, W.; Leen, V.; Dehaen, W.; Cui, J.; Xu, C.; Tang, X.; Liu, W.; Rohand, T.; Beljonne, D.; Averbeke, B. V.; Clifford, J. N.; Driesen, K.; Binnemans, K.; Auweraer, M. V. D.; Boens, N. *J. Phys. Chem. C* **2009**, *113*, 11731–11740.
18. Qin, W.; Leen, V.; Rohand, T.; Dehaen, W.; Dedecker, P.; Van der Auweraer, M.; Robeyns, K.; Van Meervelt, L.; Beljonne, D.; Van Averbeke, B.; Clifford, J. N.; Driesen, K.; Binnemans, K.; Boens, N. *J. Phys. Chem. A* **2009**, *113*, 439–447.
19. Rohand, T.; Qin, W.; Boens, N.; Dehaen, W. *Eur. J. Org. Chem.* **2006**, 4658–4663.
20. Khan, T. K.; Rao, M. R.; Ravikanth, M. *Eur. J. Org. Chem.* **2010**, 2314–2323.
21. Kee, H. L.; Kirmaier, C.; Yu, L.; Thamyongkit, P.; Youngblood, W. J.; Calder, M. E.; Ramos, L.; Noll, B. C.; Bocian, D. F.; Scheidt, W. R.; Birge, R. R.; Lindsey, J. S.; Holten, D. *J. Phys. Chem. B* **2005**, *109*, 20433–20443.
22. Kim, K.; Jo, C.; Easwaramoorthi, S.; Sung, J.; Kim, D. H.; Churchill, D. G. *Inorg. Chem.* **2010**, *49*, 4881–4894.
23. Darling, S. L.; Mak, C. C.; Bampos, N.; Feeder, N.; Teat, S. J.; Sanders, J. K. M. *New J. Chem.* **1999**, *23*, 359–364.

24. Kojima, T.; Nakanishi, T.; Honda, T.; Harada, R.; Shiro, M.; Fukuzumi, S. *Eur. J. Inorg. Chem.* **2009**, 727–734.
25. Quan-Guo, W.; Seik-Weng, N.; Wei-Hong, Z.; Yong-Shu, X. *Chin. J. Struct. Chem.* **2010**, *29*, 1197–1200.
26. Sheldrick, G. M. *SHELXS-97, Program for Crystal Structure Solution*; University of Göttingen: Göttingen, Germany, 1997.
27. Sheldrick, G. M. *SHELXL-97, Program for Crystal Structure Refinement*; University of Göttingen: Göttingen, Germany, 1997.